Inorg. Chem. **2003**, *42*, 5762–5770

Carrier-Facilitated Bulk Liquid Membrane Transport of Iron(III)–Siderophore Complexes Utilizing First Coordination Sphere Recognition

Joseph I. Wirgau and Alvin L. Crumbliss*

Department of Chemistry, Duke University, Durham, North Carolina 27708-0346

Received February 13, 2003

Carrier-facilitated bulk liquid membrane (BLM) transport from an aqueous source phase through a chloroform membrane phase to an aqueous receiving phase was studied for various hydrophilic synthetic and naturally occurring Fe(III)–siderophore complexes using first coordination sphere recognition. Iron transport systems were designed such that two cis coordination sites on a hydrophilic Fe(III) complex are occupied by labile aquo ligands, while the other four coordination sites are blocked by strong tetradentate ligands (siderophores). The labile aquo coordination sites can be "recognized" by a liquid membrane-bound hydrophobic bidentate ligand, which carries the hydrophilic Fe(III)–siderophore complex across the hydrophobic membrane to an aqueous receiving phase. The system is further designed for uphill transport of Fe(III) against a concentration gradient, driven by anti-port H^+ transport. Three tetradentate siderophore and siderophore mimic ligands were investigated: rhodotorulic acid (H_2L^{RA}), alcaligin (H_2L^{AG}), and *N*,*N*′-dihydroxy-*N*,*N*′-dimethyldecanediamide (H_2L^8). Flux values for the transport of $Fe(L^x)(OH_2)_2^+$ (x = RA, AG, 8) facilitated by the hydrophobic lauroyl hydroxamic acid (HLHA) membrane carrier were the highest when x = 8, which is attributed to substrate lipophilicity. Ferrioxamine B ($FeHDFB^+$) was also selectively transported through a BLM by HLHA. The process involves partial dechelation of ferrioxamine B to produce the tetradentate form of the complex ($Fe(H_2DFB)(OH_2)_2^{2+}$), followed by ternary complex formation with HLHA ($Fe(H_2DFB)(LHA)^+$) and transport across the membrane into the receiving phase. Uphill transport of ferrioxamine B was confirmed by increased flux as $[H^+]_{source\ phase} < [H^+]_{receiving\ phase}$. The membrane flux of ferrioxamine B occurs near neutral pH, as evidence that ternary complex formation and ligand exchange are viable processes at the membrane/receptor surface of microbial cells.

Introduction

Siderophore-mediated iron uptake is a complex process which varies between different microbes.[1] Siderophores are low-molecular-weight organic compounds that serve to selectively bind and solubilize iron in a multistep process.[2−5] First, the siderophore is synthesized and released by the cell; the siderophore then must chelate iron, forming an iron−siderophore complex. The iron−siderophore complex then diffuses to the surface of the cell where it is recognized by a membrane receptor. Once recognized, the iron is transported through the cell membrane, in some cases as the intact iron−siderophore complex, while in others the iron is released to a membrane-bound carrier. Finally, iron is released to the cell interior, where it is used in various essential metabolic functions.

Although this broad scheme can be used to generally describe siderophore-mediated microbial iron acquisition, many aspects of the mechanism of the individual steps are not understood. One of the challenges is that a single mechanism is not applicable to all microbes. Evidence of the complexity and variability of the mechanism for microbial iron acquisition may be seen in recent reports[6] that the outer membrane receptor FpvA in *Pseudomonas aeruginosa*

* To whom correspondence should be addressed. Fax: 919-660-1605. E-mail: alvin.crumbliss@chem.duke.edu.

(1) Drechsel, H.; Winkelmann, G. In *Transition Metals in Microbial Metabolism*; Winklemann, G., Carrano, C. J., Eds.; Harwood: Amsterdam, 1997; pp 1−49.
(2) Raymond, K. N.; Telford, J. R. *NATO ASI Ser., Ser. C* **1995**, *459*, 25−37.
(3) Albrecht-Gary, A.-M.; Crumbliss, A. L. *Met. Ions Biol. Syst.* **1998**, *35*, 239−327.
(4) Boukhalfa, H.; Crumbliss, A. L. *BioMetals* **2002**, *15*, 325−339.
(5) Stintzi, A.; Raymond, K. N. In *Molecular and Cellular Iron Transport*; Templeton, D. M., Ed.; Marcel Dekker: New York, 2002; pp 273−320.

10.1021/ic034157e CCC: $25.00
Published on Web 08/14/2003

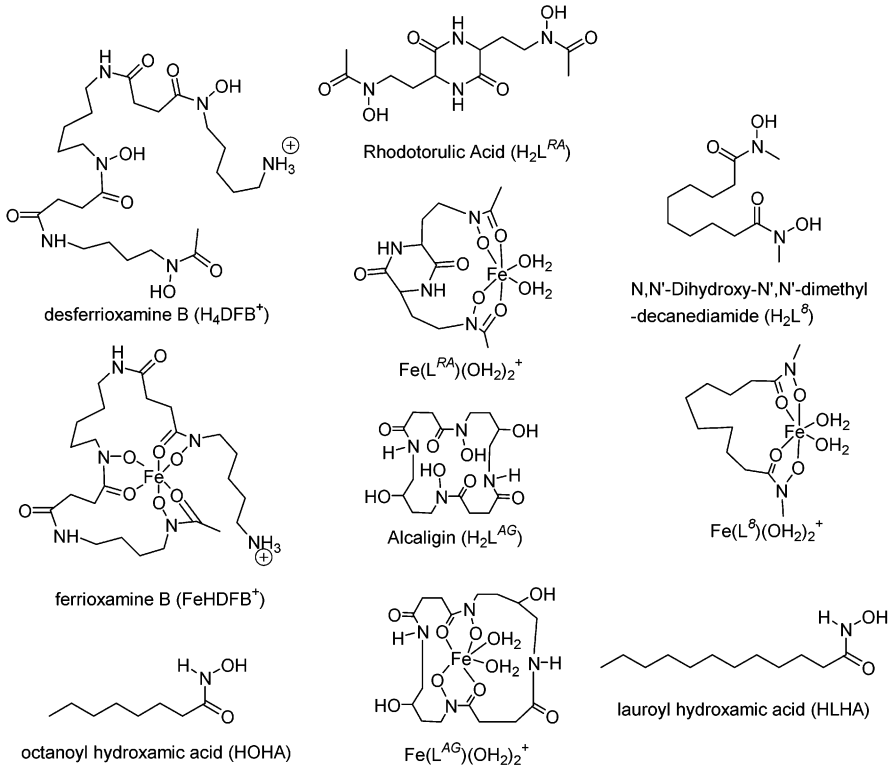

Figure 1. Structures of naturally occurring hydroxamic acid siderophores and a synthetic mimic used in this study.

binds iron-free pyoverdin and that iron transport through the membrane involves displacement of the apo-siderophore by the Fe(III)-bound form.[7,8] Another recent report describes a shuttle mechanism for membrane iron transport in *Aeromonas hydrophila*,[9] which proposes Fe(III) exchange between a number of environmental siderophore carriers and an apo-siderophore bound to an outer membrane receptor. This event is followed by a receptor conformational change and transport of the iron−siderophore complex into the cell. Further evidence of microbial iron acquisition diversity comes from characterization of the over 20 separate outer membrane ferric siderophore receptor proteins (FSRP) identified for the recognition and transport of iron−siderophore complexes through the outer membrane.[10,11] Gram-negative bacteria are capable of producing multiple FSRPs, even producing FSRPs specific for siderophores produced by other bacteria.[12] Many of the FSRPs are selective for more than one iron−siderophore complex,[13] and a current approach to the development of new antibiotics takes advantage of this fact by using compounds that will be transported into bacteria through specific FSRP.[14] However, despite diversity in the individual mechanisms, there are still features common to multiple microbes. FSRPs are only expressed at high levels in iron-deficient media, and they all exhibit a TonB dependence.[10,11]

Desferrioxamine B (H_4DFB^+; Figure 1) is a linear trihydroxamic acid siderophore produced by some species of *Nocardia* and *Streptomyces*,[15] whose Fe(III) complex ($FeHDFB^+$; Figure 1) crystal structure has recently been determined.[16] The lipophilicity of H_4DFB^+ and $FeHDFB^+$ may be increased through the attachment of a lipophilic molecule, such as an ionophore. Noncovalent attachment of an assortment of ionophores to ferrioxamine B has been previously described in terms of host−guest complexation in the second coordination shell.[17−25] Some of these systems

(6) Dhungana, S.; Crumbliss, A. L. *Chemtracts* **2001**, *14*, 258−265.
(7) Schalk, H.; Kyslik, P.; Prome, D.; van Dorsselaer, A.; Poole, K.; Abdallah, M. A.; Pattus, F. *Biochemistry* **1999**, *38*, 9357−9365.
(8) Schalk, I. J.; Hennard, C.; Dugave, C.; Poole, K.; Abdallah, M. A.; Pattus, F. *Mol. Microbiol.* **2001**, *39*, 351−360.
(9) Stintzi, A.; Barnes, C.; Xu, J.; Raymond, K. N. *Proc. Natl. Acad. Sci USA* **2000**, *97*, 10691−10696.
(10) van der Helm, D. *Met. Ions Biol. Syst.* **1998**, *35*, 355−401.
(11) Clarke, T. E.; Tari, L. W.; Vogel, H. J. *Curr. Top. Med. Chem.* **2001**, *1*, 7−30.
(12) Yun, C. W.; Ferea, T.; Rashford, J.; Ardon, O.; Brown, P. O.; Botstein, D.; Kaplan, J.; Philpott, C. C. *J. Biol. Chem.* **2000**, *275*, 10709−10715.
(13) Ferguson, A. D.; Hofmann, E.; Coulton, J. W.; Diederichs, K.; Welte, W. *Science* **1998**, *282*, 2215−2220.
(14) Braun, V. *Drug Resistance Updates* **1999**, *2*, 363−369.
(15) Mueller, G.; Raymond, K. N. *J. Bacteriol.* **1984**, *160*, 304−312.
(16) Dhungana, S.; White, P. S.; Crumbliss, A. L. *J. Biol. Inorg. Chem.* **2001**, *6*, 810−818.
(17) Batinić-Haberle, I.; Crumbliss, A. L. *Inorg. Chem.* **1995**, *34*, 928−932.
(18) Batinić-Haberle, I.; Spasojević, I.; Crumbliss, A. L. *Inorg. Chem.* **1996**, *35*, 2352−2359.
(19) Batinić-Haberle, I.; Spasojević, I.; Crumbliss, A. L. *Inorg. Chim. Acta* **1997**, *260*, 35−41.
(20) Batinić-Haberle, I.; Spasojević, I.; Jang, Y.; Bartsch, R. A.; Crumbliss, A. L. *Inorg. Chem.* **1998**, *37*, 1438−1445.
(21) Caldwell, C. D.; Crumbliss, A. L. *Inorg. Chem.* **1998**, *37*, 1906−1912.
(22) Crumbliss, A. L.; Batinić-Haberle, I.; Spasojević, I. *Pure Appl. Chem.* **1996**, *68*, 1225−1230.
(23) Spasojević, I.; Batinić-Haberle, I.; Choo, P. L.; Crumbliss, A. L. *J. Am. Chem. Soc.* **1994**, *116*, 5714−5721.
(24) Trzaska, S. M.; Toone, E. J.; Crumbliss, A. L. *Inorg. Chem.* **2000**, *39*, 1071−1075.
(25) Trzaska, S. M.; Kim, M.; Bartsch, R. A.; Crumbliss, A. L. *Inorg. Chem.* **2001**, *40*, 5823−5828.

were also utilized in bulk liquid membrane (BLM) transport experiments.[26−28]

This report expands on our previous work by covalently binding lipophilic hydroxamic acids directly to an iron−siderophore complex and transporting the resulting ternary complex across a BLM. We term this process BLM transport facilitated by first coordination sphere recognition. This is in contrast to our previous BLM transport experiments, which rely on second coordination sphere recognition.[26−28] The efficiency of carrier-facilitated BLM transport via first coordination sphere recognition will be established in this report by using two types of substrate complexes. The first are Fe(III) complexes with labile aquated coordination sites ($Fe(L^x)(OH_2)_2^+$) utilizing natural siderophore ligands such as rhodotorulic acid (isolated from *Rhodotorula pilimanae*,[29−33] H_2L^{RA}; Figure 1) and alcaligin (isolated from *Alcaligenes denitrificans* KN3-J, *Alcaligens xylosoxidans*, *Bordetella pertussis*, and *Bordetella bronchiseptica*,[34−37] H_2L^{AG}; Figure 1) and the synthetic siderophore mimic *N*,*N*′-dihydroxy-*N*,*N*′-dimethyldecanediamide (H_2L^8; Figure 1). The second type are substrate complexes with labile aquated coordination sites that are controlled by pH, such as ferrioxamine B. Both systems of substrate complexes use the hydrophobic lauroyl hydroxamic acid (HLHA) or octanoyl hydroxamic acid (HOHA) as a membrane carrier and rely upon Fe(III) first coordination shell recognition and ternary complex formation to facilitate BLM transport.

A pH gradient across the membrane provides a mechanism for the "uphill" (against a concentration gradient) transport of the Fe(III)−siderophore complexes with anti-port H^+ transport. This allows for the efficient and complete compartmentalization of iron.

While this system is significant for modeling microbial iron uptake, it has further environmental implications. Metal pollution is an ever more important problem with over two-thirds of all Superfund and DOD sites and roughly half of all RCRA and DOE sites requiring remediation for different types of metal contamination.[38] On the basis of the chemistry presented here, it is possible to conceptualize a system in which a hazardous metal is chelated by a lipophilic carrier molecule and concentrated into a solution for eventual compartmentalization and waste cleanup. An applicable lipophilic carrier molecule would exhibit metal selectivity and variable chelation strength that could be modulated by specific parameters, such as, pH, ionic strength, and temperature.

Experimental Section

Materials. Chloroform (Mallinckrodt ChromAR, HPLC grade) was used for the liquid membrane, $Mg(ClO_4)_2$ (Perkin-Elmer) was used for ionic strength control, and $Mg(OH_2)_2$ (Aldrich) and $HClO_4$ (Fisher, 70%) were used to adjust pH. All aqueous solutions were prepared with deionized water, and the pH was measured with a Corning 250 pH/ion meter equipped with an Orion ROSS pH electrode filled with a 3.0 M NaCl solution.

N,*N*′-Dihydroxy-*N*,*N*′-dimethyldecanediamide (H_2L^8), alcaligin (H_2L^{AG}), and rhodotorulic acid (H_2L^{RA}, Aldrich) were prepared and characterized as previously described.[37,39−42] A ferrioxamine B ($FeHDFB^+ClO_4^-$) stock solution was prepared as previously described.[26] Lauric acid (Aldrich, 99.5+%) was used as obtained. Lauroyl hydroxamic acid (HLHA, $HN(OH)C(=O)(CH_2)_{10}CH_3$) and octanoyl hydroxamic acid (HOHA, $HN(OH)C(=O)(CH_2)_6CH_3$) were prepared by reacting the appropriate acid chloride with hydroxylamine in the presence of aqueous sodium bicarbonate at 0 °C under a N_2 atmosphere.[40]

Methods. Aqueous solutions of $Fe(L^x)(OH_2)_2^+$ were prepared by dissolving an equimolar amount of H_2L^x (x = 8, RA, AG) in an aqueous solution containing 0.112 M $Fe(ClO_4)_3$ at pH 1.0 and diluting to volume with 0.1 M $Mg(ClO_4)_2$. $Mg(OH)_2$ was added to adjust the pH, and the solution was filtered and characterized spectrophotometrically (λ_{max} = 470 nm, ϵ_{max} = 1500−1900 cm^{-1} M^{-1}).[42] BLM transport experiments were carried out in a U-shaped spectrophotometer cell fabricated in house.[26,27] Reproducible stirring and geometric consistency were utilized to minimize scatter in the flux data. Stir speeds were kept constant at 960 rpm by a continuous-duty synchronous AC motor. Continuous absorbance readings of all three phases (source, membrane, and receiving) were obtained using a Beckman Acta III double-beam UV−vis spectrophotometer. The membrane layer consists of 4 mL of chloroform, and the receiving and source phases each consist of 2 mL of aqueous solution that were pipetted simultaneously into the cell. Flux values were calculated in units of mol cm^{-2} s^{-1} from the initial slopes of the absorbance versus time traces. Data points in flux figures represent the average of one to three individual replications. Uncertainties in individual flux values range from 5% at small values to 10% at larger values. A brief (ca. 40 min) induction period occurs while the solutions at the "membranes" (unstirred layers) reach steady-state conditions, and initial flux rates do not include the data from this nonlinear induction period. Absorbance traces also deviate from linearity after an extended period of time when the concentration in the source phase becomes depleted. Additional details are reported elsewhere.[26,27]

(26) Spasojević, I.; Crumbliss, A. L. *J. Chem. Soc., Dalton Trans.* **1998**, 4021−4028.
(27) Spasojević, I.; Crumbliss, A. L. *Inorg. Chem.* **1999**, *38*, 3248−3250.
(28) Wirgau, J. I.; Crumbliss, A. L. Accepted for publication in *J. Chem. Soc., Dalton Trans.*
(29) Carrano, C. J.; Cooper, S. R.; Raymond, K. N. *J. Am. Chem. Soc.* **1979**, *101*, 599−604.
(30) Carrano, C. J.; Raymond, K. N. *J. Bacteriol.* **1978**, *136*, 69−74.
(31) Mueller, G.; Barclay, S. J.; Raymond, K. N. *J. Biol. Chem.* **1985**, *260*, 13916−13920.
(32) Mueller, G.; Isowa, Y.; Raymond, K. N. *J. Biol. Chem.* **1985**, *260*, 13921−13926.
(33) Atkin, C. L.; Neilands, J. B. *Biochemistry* **1968**, *7*, 3734−3739.
(34) Nishio, T.; Ishida, Y. *Agric. Biol. Chem.* **1990**, *54*, 1837−1839.
(35) Nishio, T.; Tanaka, N.; Hiratake, J.; Katsube, Y.; Ishida, Y.; Oda, J. *J. Am. Chem. Soc.* **1988**, *110*, 8733−8734.
(36) Moore, C. H.; Foster, L. A.; Gerbig, D. G., Jr.; Dyer, D. W.; Gibson, B. W. *J. Bacteriol.* **1995**, *177*, 1116−1118.
(37) Brickman, T. J.; Hansel, J.-G.; Miller, M. J.; Armstrong, S. K. *BioMetals* **1996**, *9*, 191−203.
(38) Abbreviations: DOD, Department of Defense; DOE, Department of Energy; RCRA, Resource Conservation and Recovery Act; Superfund, commonly used name for the Federal Comprehensive Environmental Response, Compensation and Liability Act (CERCLA).
(39) Das, M. K.; Bose, P.; Roy, N. *J. Chem. Eng. Data* **1984**, *29*, 345−348.
(40) Smith, W. L.; Raymond, K. N. *J. Am. Chem. Soc.* **1980**, *102*, 1252−1255.
(41) Caudle, M. T.; Cogswell, L. P.; Crumbliss, A. L. *Inorg. Chem.* **1994**, *33*, 4759−4773.
(42) Boukhalfa, H.; Brickman, T. J.; Armstrong, S. K.; Crumbliss, A. L. *Inorg. Chem.* **2000**, *39*, 5591−5602.

Scheme 1

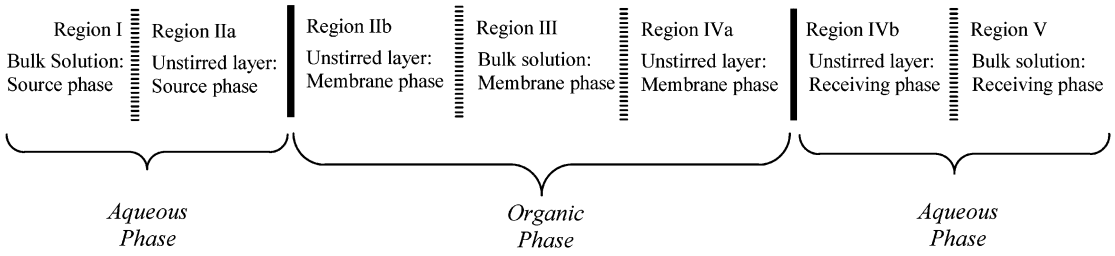

Results

General Considerations. BLM transport experiments contain three phases which can be further broken down into seven regions (Scheme 1). Relative concentrations can be assigned to each region during the process of a species (M) being transported from region I to region V in Scheme 1. The concentration of M is constant throughout region I due to stirring but decreases through region IIa as M is extracted into region IIb, causing an initial concentration jump in region IIb. As the distance from the interface of region IIa and region IIb increases, the concentration of M drops in region IIb until it enters region III and becomes constant, due to stirring. Region IVa is analogous to region IIa, as the concentration drops until the interface with region IVb, followed by an abrupt drop in concentration as M enters into the dilute receiving phase (regions IVb and V). Regions II (IIa and IIb) and IV (IVa and IVb) consist of the unstirred layers and represent "membranes"[43] with an estimated thickness between 50 and 300 μM,[26] roughly 20 000 times the size of a microbial membrane (5 nm).[44]

The basis for first coordination sphere recognition in our experiments is the existence of two cis labile coordination sites on the Fe(III) center. Both hydrophobic membrane carriers, lauroyl hydroxamic acid (HLHA, HN(OH)C(=O)-$(CH_2)_{10}CH_3$; Figure 1) and octanoyl hydroxamic acid (HOHA, HN(OH)C(=O)$(CH_2)_6CH_3$; Figure 1), are bidentate ligands and therefore need at least two coordination sites to recognize an Fe^{3+} ion or complex. In the $Fe(L^x)(OH_2)_2^+$ complex (x = AG, RA, 8) the tetradentate ligand ($L^{x\,2-}$) acts to block four coordination sites, leaving two coordination sites occupied by labile water ligands, thus satisfying the requirement for available/labile coordination sites (Figure 1).[45−49] The source of lability for the coordinated waters is the increased rate of water exchange for the $Fe(L^x)(OH_2)_2^+$ complexes relative to $Fe(OH_2)_6^{3+}$.[3,50,51] First coordination shell recognition and membrane transport occur through lipophilic ternary complex formation, as illustrated in reaction 1 (R = $-(CH_2)_6CH_3$, $-(CH_2)_{10}CH_3$).

$$\{Fe(L^x)(OH_2)_2^+\}_{aq} + \{HN(OH)C(=O)R\}_{org} \rightleftarrows \{Fe(L^x)(HN(O)C(=O)R)\}_{org} + H_3O^+ + H_2O \quad (1)$$

In ferrioxamine B two iron coordination sites can be aquated by partial dissociation of the ferrioxamine B chelate ring (reaction 2; log K = 0.94 (52)), a process that is controlled by solution pH. At lower pH values the tris-

$$FeHDFB^+ + H_3O^+ + H_2O \rightleftarrows Fe(H_2DFB)(OH_2)_2^{2+} \quad (2)$$

(hydroxamate) complex will begin to dissociate and the fraction of desferrioxamine B acting as a tetradentate ligand increases. The tetradentate form of the complex can accept an incoming ligand to form a lipophilic ternary complex (eq 3; R = $-(CH_2)_{10}CH_3$)), capable of transport across a chloroform membrane phase, along with its counteranion.

$$\{Fe(H_2DFB)(OH_2)_2^{2+}\}_{aq} + {ClO_4^-}_{aq} + \{HN(OH)C(=O)R\}_{org} \rightleftarrows \{Fe(H_2DFB)(HN(O)C(=O)R)^+, ClO_4^-\}_{org} + {H_3O^+}_{aq} + H_2O \quad (3)$$

Comparison of Membrane Carriers HLHA and HOHA. Two lipophilic mono(hydroxamic acids) were investigated with respect to their ability to transport $Fe(L^x)(OH_2)_2^+$ (x = AG, RA, 8) through a chloroform bulk liquid membrane. Both carriers were effective, with flux values for HOHA slightly higher than for HLHA under identical conditions (Figure 2). This is attributed to the slight solubility of HOHA in water, whereas HLHA has no measurable solubility in aqueous solutions. HLHA was used for the detailed flux measurements reported here instead of HOHA, due to the importance of restricting the carrier to the membrane phase.

Influence of pH. BLM transport of $Fe(L^x)(OH_2)_2^+$ using HOHA and HLHA is sensitive to the pH in both the receiving and source phases. The top two curves of Figure 2 represent flux data sets for $Fe(L^8)(OH_2)_2^+$ using HOHA as the carrier with source phase pH 5.0 (top curve) and 2.4 (middle curve).

(43) Visser, H. C.; Reinhoudt, D. N.; de Jong, F. *Chem. Soc. Rev.* **1994**, *23*, 75−81.
(44) Alberts, B.; Bray, D.; Lewis, J.; Raff, M.; Roberts, K.; Watson, J. D. *Molecular Biology of the Cell*; Garland: New York, 1989.
(45) A cis geometry for the coordinated aquo ligands is required for the first coordination sphere recognition process described here. Crystallographic data are available for $Fe(L^{AG})(OH_2)_2$, which demonstrate a cis geometry.[46] Crystal structures are not available for $Fe(L^{RA})(OH_2)_2$ or $Fe(L^8)(OH_2)_2$, although ESI-MS data confirm that under our conditions these complexes exist as monoiron as opposed to diiron species and are most likely in cis configurations for steric reasons.[47−49]
(46) Hou, Z.; Sunderland, C. J.; Nishio, T.; Raymond, K. N. *J. Am. Chem. Soc.* **1996**, *118*, 5148−5149.
(47) Caudle, M. T.; Stevens, R. D.; Crumbliss, A. L. *Inorg. Chem.* **1994**, *33*, 6111−6115.
(48) Caudle, M. T.; Stevens, R. D.; Crumbliss, A. L. *Inorg. Chem.* **1994**, *33*, 843−844.
(49) Spasojević, I.; Boukhalfa, H.; Stevens, R. D.; Crumbliss, A. L. *Inorg. Chem.* **2001**, *40*, 49−58.
(50) Swaddle, T. W.; Merbach, A. E. *Inorg. Chem.* **1981**, *20*, 4212−4216.
(51) Biruš, M.; Kujundžić, N.; Pribanić, M. *Prog. React. Kinet.* **1993**, *18*, 173−271.

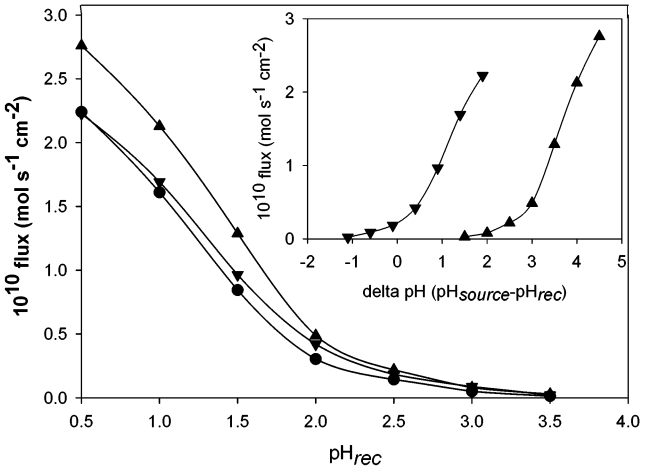

Figure 2. Flux of $Fe(L^8)(OH_2)_2^+$ with HLHA and HOHA carriers as a function of the aqueous receiving phase pH, and with HOHA carrier as a function of the difference in aqueous source and receiving phase pH (inset): (▲) $[HOHA]_{mem}$ = 1.5 mM and pH_{source} 5.0; (▼) $[HOHA]_{mem}$ = 1.5 mM and pH_{source} 2.4; (●) $[HLHA]_{mem}$ = 1.5 mM and pH_{source} 2.4. Source phase conditions: 0.1 M $Mg(ClO_4)_2$, 1.5 mM $Fe(L^8)(OH_2)_2^+$, pH 2.4 or 5.0. Membrane phase conditions: 1.5 mM HLHA or HOHA. Receiving phase conditions: 0.1 M $Mg(ClO_4)_2$, pH 0.5−3.5. Solid lines are drawn to show trends in the data.

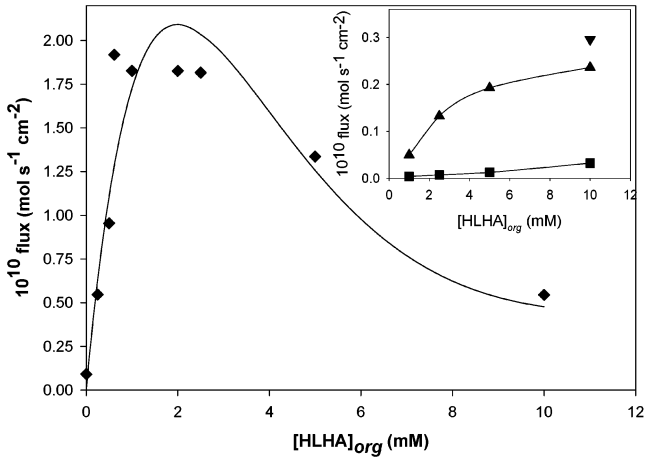

Figure 3. Flux of $Fe(L^x)(OH_2)_2^+$ as a function of lauroyl hydroxamic acid (HLHA) membrane carrier concentration, where $L^x = L^8$, L^{RA} (inset), L^{AG} (inset): (♦) $Fe(L^8)(OH_2)_2^+$ and pH_{source} 2.2; (▼) $Fe(L^{AG})(OH_2)_2^+$ and pH_{source} 4.8; (▲) $Fe(L^{RA})(OH_2)_2^+$ and pH_{source} 4.8; (■) $Fe(L^{RA})(OH_2)_2^+$ and pH_{source} 2.2. Source phase conditions: 0.1 M $Mg(ClO_4)_2$, 1.5 mM $Fe(L)(OH_2)_2^+$, pH 2.2 or 4.8. Membrane phase conditions: $[HLHA]_{mem}$ = 0−10 mM. Receiving phase conditions: 0.1 M $Mg(ClO_4)_2$, pH 0.5. Solid lines are drawn to show the trends in the data.

Over the pHs investigated, the flux is greater with a higher pH in the source phase and a lower pH in the receiving phase. UV−vis spectra of all three phases were obtained at the conclusion of each transport experiment. The wavelength maximum was 428 nm in the membrane phase and 467 nm in both the source and receiving phases, consistent with tris(hydroxamate) coordination, $Fe(L^8)(HN(O)C(=O)R)$, and bis(hydroxamate) coordination, $Fe(L^8)(OH_2)_2^+$, respectively.[53]

The data presented in Figure 2 are consistent with antiport proton transport; i.e., H^+ ions are transported in the opposite direction as the Fe(III) complex. Under conditions where $pH_{receiving} < pH_{source}$, the excess $[H^+]$ in the receiving phase is used to drive the transport of $Fe(L^8)(OH_2)_2^+$ "uphill" against a concentration gradient. Figure S1 (Supporting Information) presents absorbance traces as a function of time for all three phases (aqueous source, organic membrane, aqueous receiving) for a BLM transport experiment, where the initial concentration of $Fe(L^8)(OH_2)_2^+$ is the same in the aqueous source and receiving phases; $[Fe(L^8)(OH_2)_2^+]_{aq\ source} = [Fe(L^8)(OH_2)_2^+]_{aq\ rec}$. $Fe(L^8)(OH_2)_2^+$ is transported against a concentration gradient ("uphill"), and after 3 h less than 1% of the original complex remains in the source phase.

BLM Transport of $Fe(L^x)(OH_2)_2^+$ (x = AG, RA, 8) by HLHA. BLM transport flux for $Fe(L^x)(OH_2)_2^+$ (x = AG, RA, 8) was found to vary with the concentration of HLHA in the membrane phase at constant pH and ionic strength (Figure 3). For $Fe(L^{RA})(OH_2)_2^+$ and $Fe(L^{AG})(OH_2)_2^+$ the flux increased with $[HLHA]_{org}$ up to 10 mM, the concentration range covered. For $Fe(L^8)(OH_2)_2^+$ the flux increased to a maximum at $[HLHA]_{org} \approx 1.5-2.0$ mM, followed by a decrease over the concentration range investigated. The concentration of the $Fe(L^8)(LHA)$ ternary complex was recorded as a function of time in the membrane phase at various membrane phase HLHA concentrations and displayed two distinct profiles (Figure S2, Supporting Information). Data at low $[HLHA]_{org}$ exhibit a saturation profile, while at high $[HLHA]_{org}$ a steady buildup of iron complex concentration is observed in the membrane phase.

A low level of transport was observed for $Fe(L^8)(OH_2)_2^+$ in the absence of a carrier, probably due to some degree of hydrolysis to form the more hydrophobic species $Fe(L^8)(OH_2)(OH)$ ($pK_a(Fe(L^8)(OH_2)_2^+) = 6.36$).[54] This is consistent with the observation that a background flux increases with increasing source phase pH.[55]

The BLM transport of both $Fe(L^{RA})(OH_2)_2^+$ and $Fe(L^{AG})(OH_2)_2^+$ facilitated by the carrier HLHA show appreciable flux values, even at low HLHA concentrations (Figure 3). When the pH of the source phase was increased (all other variables held constant) from 2.2 to 4.8 for the $Fe(L^{RA})(OH_2)_2^+$ system, the flux rates increased by approximately 1 order of magnitude (data not shown). Figure 3 illustrates a modest increase in flux for $Fe(L^{AG})(OH_2)_2^+$ relative to $Fe(L^{RA})(OH_2)_2^+$. As was observed with $Fe(L^8)(OH_2)_2^+$, transport of both $Fe(L^{AG})(OH_2)_2^+$ and $Fe(L^{RA})(OH_2)_2^+$ occurred against a concentration gradient and UV−vis spectra of the membrane and receiving phases demonstrate wavelength maxima at 428 and 467 nm respectively. The

(52) Schwarzenbach, G.; Schwarzenbach, K. *Helv. Chim. Acta* **1963**, *46*, 1390−1400.
(53) Caudle, M. T.; Crumbliss, A. L. *Inorg. Chem.* **1994**, *33*, 4077−4085.
(54) Caudle, M. T.; Caldwell, C. D.; Crumbliss, A. L. *Inorg. Chim. Acta* **1995**, *240*, 519−525.
(55) For a series of experiments with a source phase containing 1.5 mM $FeL^8(OH_2)_2^+$ and 0.1 M $Mg(ClO_4)_2$ and a receiving phase containing 0.1 M $Mg(ClO_4)_2$ at pH 1.0, the following background flux values were obtained at various source phase pH values (flux, mol s^{-1} cm^{-2}; source phase pH): 0.14×10^{-10}, 2.0; 0.17×10^{-10}, 3.0; 0.24×10^{-10}, 4.0; 0.37×10^{-10}, 5.0. In these experiments the spectrum of the membrane phase shows λ_{max} = 421 nm (ϵ = [1.54(5)] × 10^3 cm^{-1} M^{-1}), consistent with the presence of $Fe(L^8)(OH_2)(OH)$ in the membrane phase. This background flux represents from 8 to 28% of the measured fluxes reported here for first coordination shell carrier-facilitated membrane transport.

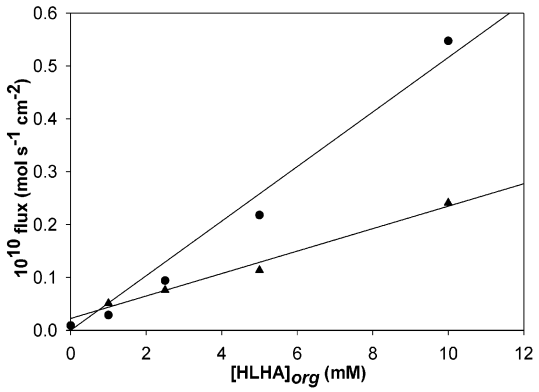

Figure 4. Flux of ferrioxamine B as a function of lauroyl hydroxamic acid (HLHA) membrane carrier concentration: (●) pH_{rec} 0.5; (▲) pH_{rec} 7.4. Solid lines represent the linear regression fit to the data points. Source phase conditions: 0.1 M $Mg(ClO_4)_2$, 50 mM $Fe(HDFB)^+$, pH 2.0. Membrane phase conditions: [HLHA] = 0−10 mM. Receiving phase conditions: 0.1 M $Mg(ClO_4)_2$, pH 0.5 or 7.4.

absorbance versus time trace of the membrane phase for the transport of the $Fe(L^{RA})(OH_2)_2^+$ (Figure S3, Supporting Information) resulted in the buildup of iron in the membrane phase with no leveling off.

BLM Transport of Ferrioxamine B by HLHA. In contrast to H_2L^{RA}, H_2L^{AG}, and H_2L^8, H_4DFB^+ is a hexadentate ligand which fully satisfies all of the coordination sites of Fe(III), leaving no labile aquated coordination sites for the formation of a ternary complex. At very low pH values the $Fe(HDFB)^+$ complex completely dissociates in a four-step process.[56−58] Ligand dissociation will partially proceed at pH 2 so that 3.6% of the ferrioxamine B will be present as the tetracoordinate species, providing an Fe(III) complex with two labile water molecules present for first coordination sphere recognition (eqs 2 and 3). Measurable fluxes are obtained at $[FeHDFB^+]_{aq\ source}$ = 50 mM and physiological pH in the receiving phase, although higher values were obtained when the receiving phase was more acidic (Figure 4). The influence of source phase pH on the flux was examined and exhibited a modest increase with increasing pH (Figure S4, Supporting Information). Absorbance readings in the membrane phase showed a buildup of Fe(III) in the membrane phase. The influence of the identity of the Fe(III) chelating group (recognition agent) of the carrier was examined by comparing flux rates for HLHA and the parent carboxylic acid, lauric acid, under identical conditions (Figure S5, Supporting Information; $[carrier]_{org}$ = 1.5 mM, pH_{source} 3.0, pH_{rec} 1.0−3.2, $[Fe(HDFB)^+]_{aq\ source}$ = 25 mM, $[Mg(ClO_4)_2]_{aq}$ = 0.1 M). The fluxes with HLHA as the carrier range from >3 to >5 times greater than for the corresponding values using lauric acid. In addition to having larger flux values, the experiments with HLHA as the carrier exhibited a pH dependence with the highest flux at the lowest receiving phase pH values, indicative of anti-port H^+ transport. The experiments with lauric acid showed no pH dependence. No flux of $FeHDFB^+$ or any of its partially hydrolyzed species was observed in the absence of a carrier. These data support $FeHDFB^+_{aq}$ BLM transport through lipophilic ternary complex formation, $Fe(H_2DFB)(LHA)^+$, and not ion pairing.

Discussion

First Coordination Shell Recognition and Transport of $Fe(L^x)(OH_2)_2^+$ (x = AG, RA, 8). The overall flux under a given set of conditions depends on the thermodynamics of the extraction of the substrate of interest from the source phase (Scheme 1, regions I and IIa) into the membrane phase (Scheme 1, regions IIb, III, and IVa) and the back-extraction from the membrane phase into the receiving phase (Scheme 1, regions IVb and V). Equations 4−6 describe the extraction of $Fe(L^x)(OH_2)_2^+$ by HLHA into the membrane phase, where $L^{x\ 2-}$ represents $L^{RA\ 2-}$, $L^{AG\ 2-}$, and $L^{8\ 2-}$.[23]

$$Fe(L^x)(OH_2)_2^{+}{}_{aq} + ClO_4^{-}{}_{aq} + HLHA_{org} \overset{K_{ex}'}{\rightleftharpoons} Fe(L^x)(LHA)_{org} + HClO_{4\ aq} + 2H_2O_{aq} \quad (4)$$

$$Fe(L^x)(OH_2)_2^{+}{}_{aq} + ClO_4^{-}{}_{aq} \overset{K_d'}{\rightleftharpoons} Fe(L^x)(OH_2)_2^{+}ClO_4^{-}{}_{org} \quad (5)$$

$$Fe(L^x)(OH_2)_2^{+}ClO_4^{-}{}_{org} + HLHA_{org} \overset{K_a'}{\rightleftharpoons} Fe(L^x)(LHA)_{org} + HClO_{4\ aq} + 2H_2O_{aq} \quad (6)$$

$$K_{ex}' = K_d' K_a' \quad (7)$$

The extraction of the iron complex into the membrane phase (eq 4) is dependent upon two steps. The first is an ion-pairing or distribution process (eq 5), which is primarily driven by the lipophilicity of both the complex and the counterion. The second step is ternary complex formation dependent on the equilibrium described by eq 6. When the distribution and ternary complex formation equilibria (eqs 5 and 6) are established rapidly, the diffusion of the ternary complex $(Fe(L^x)(LHA)_{org}$ as presented above or $Fe(H_2DFB)(LHA)^+_{org}$ as presented below) in the unstirred portion of the membrane will control the overall flux. Under these conditions eq 8 relates the flux (mol cm^{-2} s^{-1}) to the extraction constant K_{ex}', the diffusion coefficient for the complex assembly in the membrane solvent (D_{mem}), the diffusion layer thickness in region IIb (l), the carrier concentration in the membrane phase ($[HLHA]_{org}$), and the iron complex concentration in the aqueous source phase ($[Fe(L^x)(OH_2)_2^+]_{aq\ source}$).[26]

$$flux = K_{ex}'(D_{org}/l)[HLHA]_{org}[Fe(L^x)(OH_2)_2^{+}]_{aq\ source} \quad (8)$$

The dependence of the flux on the pH of the source phase can be described as a perturbation of eq 6, which illustrates the competition of protons and Fe(III) for the hydroxamic acid carrier ligand (HLHA or HOHA). As the pH of the source phase is increased, the equilibrium shifts toward iron complex formation in the membrane phase, corresponding to a shift toward the right in eq 6, and an

(56) Monzyk, B.; Crumbliss, A. L. *J. Am. Chem. Soc.* **1982**, *104*, 4921−4929.
(57) Biruš, M.; Bradić, Z.; Krznarić, G.; Kujundžić, N.; Pribanić, M.; Wilkins, P. C.; Wilkins, R. G. *Inorg. Chem.* **1987**, *26*, 1000−1005.
(58) Batinić-Haberle, I.; Spasojević, I.; Crumbliss, A. L. *Inorg. Chem.* **1994**, *33*, 3151−3158.

increase in flux. This is consistent with the data presented in Figure 2.

For maximum flux, all of the equilibria in question must be favorable and rapidly established for large extraction of the iron complex from the aqueous source phase into the membrane phase and out of the membrane phase into the aqueous receiving phase. The dependence of flux on the pH of the receiving phase can be attributed to shifts in the equilibrium of the back-extraction into the receiving phase. At low receiving phase pH the flux values are greatest (Figure 2), as expected if ternary complex formation is responsible for the transport of $Fe(L^x)(OH_2)_2^+$. As the pH is lowered, the stability of the ternary complex decreases due to proton competition for LHA^-, as well as enhancing the proton-dependent second-order kinetics of ternary ligand dissociation. Consequently, low receiving phase pH favors increased formation of the hydrophilic $Fe(L^x)(OH_2)_2^+$ complex and, ultimately, increased flux values.

A driving force for the membrane transport process is the pH difference between the receiving and source phases, which can be used to compartmentalize iron by uphill transport. This is demonstrated in Figure S1 (Supporting Information), where the iron concentration is initially the same in both the source and receiving phases, but BLM transport still occurs against this iron concentration gradient until all (>99%) of the iron is moved into the receiving phase. When the iron complex concentration reaches a steady state in the membrane, the flux into the membrane from the source phase is balanced by an equivalent flux out of the membrane into the receiving phase. This is illustrated in Figure S1 for the region where the membrane phase absorbance is nearly constant with time (3400−4000 s), at which point the flux values are 6.8×10^{-11} and 7.8×10^{-11} mol cm^{-2} s^{-1} for entry into the receiving phase and exit from the source phase, respectively. Considering experimental uncertainty and the fact that steady-state conditions were only approximated, we can state that the flux out of the source phase and that into the receiving phase are equivalent. These data, taken with the pH dependence data, lead to Scheme 2 (counterions, ClO_4^-, have been omitted for clarity, x = 8, AG, RA, and the subscripts I, II, etc. refer to the regions defined in Scheme 1).

Scheme 2

$$Fe(L^x)(OH_2)_2{}^+{}_I \rightleftharpoons Fe(L^x)(OH_2)_2{}^+{}_{II} \quad (9)$$

$$Fe(L^x)(OH_2)_2{}^+{}_{II} + HLHA_{II} \rightleftharpoons Fe(L^x)(LHA)_{II} + H_3O^+{}_{II} + H_2O_{II} \quad (10)$$

$$Fe(L^x)(LHA)_{II} \rightleftharpoons Fe(L^x)(LHA)_{III} \quad (11)$$

$$Fe(L^x)(LHA)_{III} \rightleftharpoons Fe(L^x)(LHA)_{IV} \quad (12a)$$

$$Fe(L^x)(LHA)_{IV} + H_3O^+{}_{IV} + H_2O_{IV} \rightleftharpoons Fe(L^x)(OH_2)_2{}^+{}_{IV} + HLHA_{IV} \quad (13)$$

$$Fe(L^x)(OH_2)_2{}^+{}_{IV} \rightleftharpoons Fe(L^x)(OH_2)_2{}^+{}_{V} \quad (14)$$

Scheme 2 predicts linear or saturation behavior for $Fe(L^x)(OH_2)_2^+$ flux values with increasing $HLHA_{org}$ concentrations, as illustrated in the inset to Figure 3 for $Fe(L^{AG})(OH_2)_2^+$ and $Fe(L^{RA})(OH_2)_2^+$. The behavior illustrated in Figure 3 for $Fe(L^8)(OH_2)_2^+$ up to ~2 mM HLHA (which corresponds to an 8:3 HLHA to $Fe(L^8)(OH_2)_2^+$ molar ratio), where a maximum flux is reached, is accommodated by Scheme 2. The subsequent decrease in $Fe(L^8)(OH_2)_2^+$ flux as the carrier ligand to metal complex ratio reaches 3:1 or greater requires inclusion of eq 12b as a parallel process to eq 12a in Scheme 2. This process in eq 12b becomes

$$Fe(L^x)(LHA)_{III} + 2\ HLHA_{III} \rightleftharpoons Fe(LHA)_{3\ III} + H_2L^x{}_{III} \quad (12b)$$

increasingly efficient as the membrane HLHA concentration increases beyond the 8:3 $[HLHA]_{org}$ to $[Fe(L^8)(OH_2)_2^+]_{aq\ source}$ ratio. $Fe(LHA)_3$ is very lipophilic and will reside exclusively in the membrane phase. The absorbance vs time traces in Figure S2 add additional support for inclusion of reaction 12b in Scheme 2 at high HLHA concentrations, since $Fe(LHA)_3$ formation will create a buildup of iron in the membrane phase, as is observed. At the lowest HLHA concentration (Figure S2, dotted line) a gradual buildup is observed, followed by a leveling off after approximately 90 min. This same behavior is seen at slightly higher concentrations (Figure S2, dashed line), but at high HLHA concentrations (Figure S2, solid line) the absorbance increases steadily with time, corresponding to a buildup of $Fe(LHA)_3$ in the membrane phase.

The fact that flux data for $Fe(L^x)(OH_2)_2^+$ (x = AG, RA) do not exhibit a maximum over the HLHA concentration range used in our study suggests reaction 12b is not operative, consistent with the higher affinity of H_2L^{AG} and H_2L^{RA} for Fe(III) over that of H_2L^8. The small increase in flux for $Fe(L^{AG})(OH_2)_2^+$ over $Fe(L^{RA})(OH_2)_2^+$ may be attributed to the stronger binding affinity of alcaligin for Fe(III) (pFe 23.0 vs 21.9),[4,29,59] further minimizing competition from the nonproductive reaction (eq 12b). Differences in hydrophilicity between $Fe(L^{AG})(OH_2)_2^+$ and $Fe(L^{RA})(OH_2)_2^+$ may also be a factor.

The larger flux for $Fe(L^8)(OH_2)_2^+$ relative to $Fe(L^{RA})(OH_2)_2^+$ and $Fe(L^{AG})(OH_2)_2^+$ is likely due to the higher hydrophilicity of the latter two complexes brought about by the ligand backbone amide and hydroxyl groups. This will decrease K_d' in reaction 5 (data not shown). Ternary complex formation in reaction 6 is expected to be comparable for all three substrate complexes, which when taken with the decrease in reaction 5 leads to a decrease in K_{ex}' and consequently flux for $Fe(L^{AG})(OH_2)_2^+$ and $Fe(L^{RA})(OH_2)_2^+$ (eq 8).

First Coordination Sphere Recognition and Transport of Ferrioxamine B. The extraction process of ferrioxamine B into the membrane phase can be described

(59) Hou, Z.; Raymond, K. N.; O'Sullivan, B.; Esker, T. W.; Nishio, T. *Inorg. Chem.* **1998**, *37*, 6630−6637.

by eqs 15−17, analogous to eqs 4−6, and consequently eq 7 applies.

$$Fe(HDFB)^{+}_{aq} + ClO_4^{-}{}_{aq} + HLHA_{org} \overset{K_{ex}}{\rightleftharpoons} Fe(H_2DFB)(LHA)^{+},ClO_4^{-}{}_{org} \quad (15)$$

$$Fe(HDFB)^{+}_{aq} + ClO_4^{-}{}_{aq} \overset{K_d}{\rightleftharpoons} Fe(HDFB)^{+},ClO_4^{-}{}_{org} \quad (16)$$

$$Fe(HDFB)^{+}ClO_4^{-}{}_{org} + HLHA_{org} \overset{K_a}{\rightleftharpoons} Fe(H_2DFB)(LHA)^{+}ClO_4^{-}{}_{org} \quad (17)$$

These steps illustrate the distribution of ferrioxamine B between the source and membrane phases and ferrioxamine B ternary complex formation with HLHA in the membrane phase. The distribution of ferrioxamine B into the membrane phase is small (eq 16; $K_d = 3.1 \times 10^{-4}$ M^{-1} [23]) due to the hydrophilicity of the pendant ammonium group and the two backbone amide moieties. The ternary complex is charged, unlike the tetradentate ligands, requiring ion pairing with a hydrophilic perchlorate anion. The failure to record flux values under conditions comparable to those for the $Fe(L^x)(OH_2)_2^{+}$ systems is most likely due to the hydrophilicity of the complex along with the Fe(III) complexation competition between HLHA and the third hydroxamate group on desferrioxamine B, H_4DFB^{+}.

The pH dependence of the flux values can be used to eliminate ion pairing of LHA^{-} with ferrioxamine B as a possible parallel path to ternary complex formation. If HLHA were only acting as a lipophilic counterion (LHA^{-}), then the flux values should be independent of the pH of the source phase below pH 6. This is because 99.8% of the HLHA molecules will be protonated at pH 6 ($pK_a = 8.63$).[60] Figure S4 shows a dependence of the flux on the source phase pH. Additional evidence against ion pair formation comes from Figure S5, where lauric acid is used as a carrier. Lauric acid cannot compete with the third hydroxamate group of H_4DFB^{+} for the first coordination sphere of Fe(III). All flux values recorded using lauric acid can be attributed to ion pairing and not first coordination sphere extraction and transport. The fact that an approximately 4-fold increase in flux is observed when using HLHA and that a pH dependence is observed only for HLHA supports first coordination sphere recognition and transport (Scheme 3). There should be no pH dependence for ion pairing, since the pH is significantly lower than the pK_a values for the binding groups. Flux values should increase at lower receiving phase pH values for first coordination sphere binding, as low pH will facilitate ferrioxamine B release from the ternary complex. Scheme 3 describes the mechanism of ferrioxamine B transport via ternary complex formation with HLHA, where the subscripts correspond to the regions defined in Scheme 1.

(60) Boukhalfa, H.; Crumbliss, A. L. Unpublished observations.

Scheme 3

$$Fe(HDFB)^{+}_{I} + H_3O^{+}_{I} + H_2O_I \rightleftharpoons Fe(H_2DFB)(OH_2)_2^{2+}_{I} \quad (18)$$

$$Fe(H_2DFB)(OH_2)_2^{2+}_{II} + HLHA_{II} + ClO_4^{-}{}_{II} \rightleftharpoons Fe(H_2DFB)(LHA)^{+}ClO_4^{-}{}_{II} + H_3O^{+}_{II} + H_2O_{II} \quad (19)$$

$$Fe(H_2DFB)(LHA)^{+}ClO_4^{-}{}_{II} \rightleftharpoons Fe(H_2DFB)(LHA)^{+}ClO_4^{-}{}_{III} \quad (20)$$

$$Fe(H_2DFB)(LHA)^{+}ClO_4^{-}{}_{III} \rightleftharpoons Fe(H_2DFB)(LHA)^{+}ClO_4^{-}{}_{IV} \quad (21)$$

$$Fe(H_2DFB)(LHA)^{+}ClO_4^{-}{}_{IV} \rightleftharpoons Fe(HDFB)^{+}ClO_4^{-}{}_{IV} + HLHA_{IV} \quad (22)$$

$$Fe(HDFB)^{+}_{IV} \rightleftharpoons Fe(HDFB)^{+}_{V} \quad (23)$$

Scheme 3 is consistent with a relatively modest source phase pH dependence on the flux. Reactions 18 and 19 have opposing pH dependencies. Our experimental design is based on ferrioxamine B ring opening at low pH to create two labile coordinated water ligands on the Fe(III) center ($FeH_2DFB(OH_2)_2^{2+}$), analogous to the $Fe(L^x)(OH_2)_2^{+}$ systems. At pH 2, 3.5% of ferrioxamine B acts as a tetradentate ligand ((3.6×10^{-3})% at pH 5),[52] but low pH also makes chelation of Fe(III) by HLHA less favorable. However, the mono(hydroxamic acid) was able to compete with ferrioxamine B at higher pH values, as evidenced by the increasing flux values as the source phase pH was increased from 2.5 to 4.5. This may be attributed in part to the excess HLHA over ferrioxamine B in the membrane phase.

The receiving phase pH is important for the release of ferrioxamine B from the membrane phase. Low pH values facilitate dissociation of the $Fe(H_2DFB)(LHA)^{+}$ ternary complex to release the hydrophilic $Fe(HDFB)^{+}$ complex into the aqueous receiving phase (Figure 4). It is noteworthy that the formation of a ternary complex and transport of ferrioxamine B through an organic membrane phase occurs most readily when the source phase pH is near its physiological value (Figure S4). Furthermore, flux is appreciable at pH_{rec} 7.4 (Figure 4). Although the biological relevance of these observations remains to be established, it does confirm the viability of ligand exchange/ternary complex formation as important steps in membrane transport associated with siderophore-mediated iron bioavailability.[6−9]

Conclusions

It has been demonstrated that a variety of tetradentate and hexadentate iron complexes with labile aquated coordination sites can be transported across a hydrophobic membrane using first coordination sphere recognition by a bidentate iron chelator. These complexes can be transported against a concentration gradient to the extent that >99% of the complex can be moved from the source phase to the receiving phase. This uphill transport is driven by the pH differential between the source and receiving phases. A summary

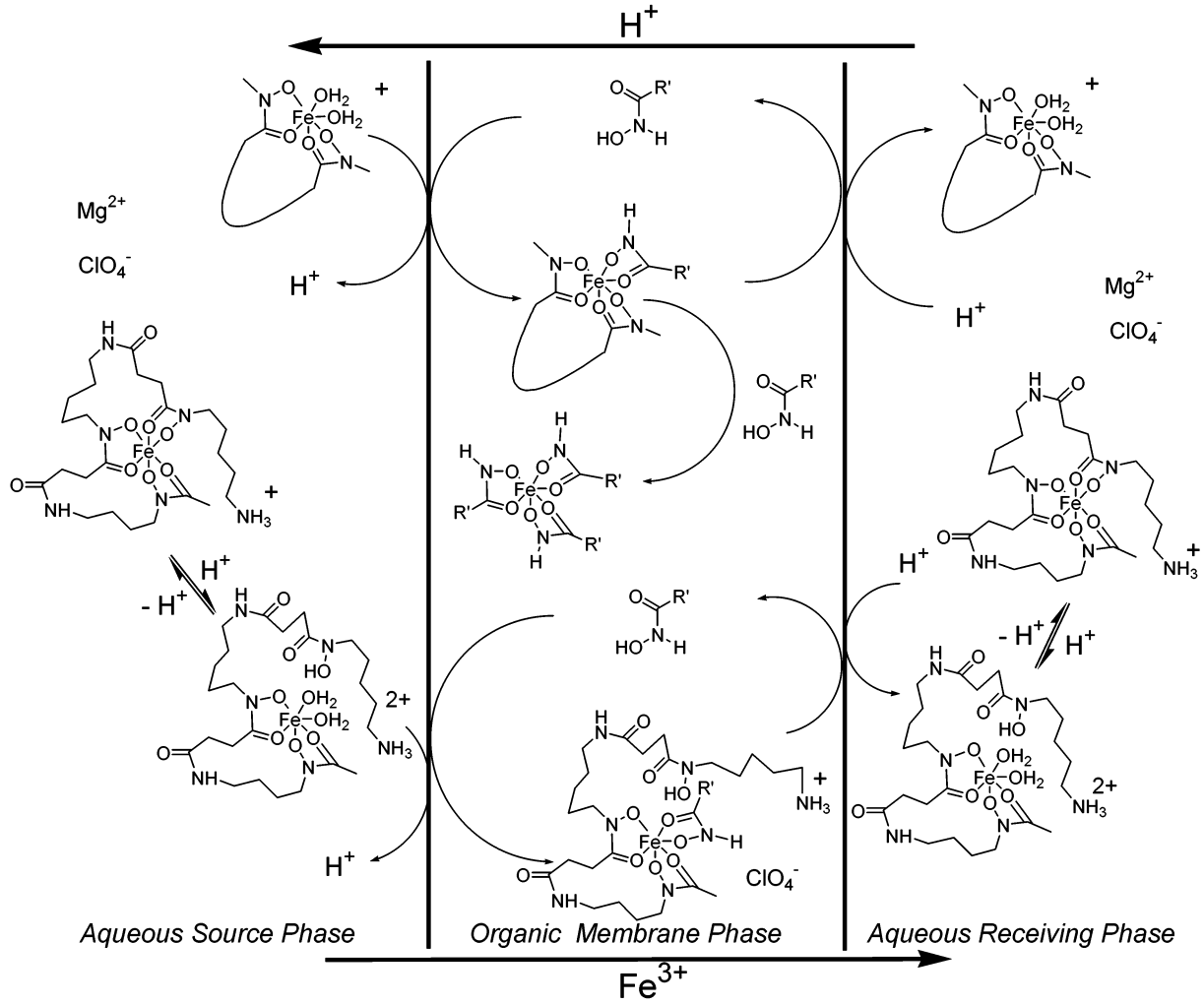

Figure 5. Summary schematic representation of carrier-facilitated BLM transport of $Fe(L^x)(OH_2)_2^+$ and $FeHDFB^+$ utilizing first coordination sphere recognition.

representation of the processes described here is presented in Figure 5. It is significant that HLHA can transport $Fe(HDFB)^+$ by first sphere recognition at nearly neutral pH. This observation lends suport to the hypothesis that in some cases ligand exchange plays a fundamental role in the mechanism of transport for iron−siderophore complexes through FSRPs.

Acknowledgment. We thank Dr. Hakim Boukhalfa, Dr. Ivan Spasojević and Prof. Richard Taylor for helpful discussions, and Prof. Sandra K. Armstrong and Dr. Timothy J. Brickman for a generous gift of alcaligin. We gratefully acknowledge the NSF (Grant No. CHE-0079066) and the donors of the Petroleum Research Fund, administered by the American Chemical Society, for financial support.

Supporting Information Available: Five figures containing flux data. This material is available free of charge via the Internet at http://pubs.acs.org.

IC034157E